

Biosynthesis of ZnO nanoparticles using *Laurus nobilis* leaf extract and investigation of antiproliferative and antibacterial activity potential

Firdevs Mert Sivri^{id1,*}, Ebru Önem^{id1}, Senem Akkoç^{id1,2}, Cennet Çırrik^{id1},
Aleyna Ezer^{id1}

¹Suleyman Demirel University, Department of Basic Pharmaceutical Sciences, 32200 Isparta, Türkiye

²Bahçeşehir University, Faculty of Engineering and Natural Sciences, Istanbul, Türkiye

Abstract: Nanotechnology has recently emerged as an essential field of study in modern materials science. The green synthesis of nanoparticles using plant extracts is of great interest because it is cost-effective, eco-friendly, and suitable for large-scale production. The study highlights the synthesis of ZnO nanoparticles (ZnO NPs) using *Laurus nobilis* (*L. nobilis*) leaf extract and their characterization and biological activities for potential applications in the biomedical field. ZnO NPs were synthesized using *Laurus nobilis* leaf extract. The synthesized ZnO NPs were characterized by UV-Vis spectroscopy, TEM, XRD, and FT-IR. According to TEM and XRD diffraction analysis, with a mean particle size of 16 ± 5 nm, it was found that the synthesized ZnO NPs contain a hexagonal wurtzite structure. ZnO NPs have antibacterial activity against Gram-positive *Staphylococcus aureus* (*S. aureus*) and Gram-negative *Escherichia coli* (*E. coli*). The antiproliferative activity of ZnO NPs was tested against the human colon cancer cell line and mouse normal fibroblast cell line using MTT assay in vitro. The results show that the prepared nanoparticles had antiproliferative in screened incubation time and concentrations.

ARTICLE HISTORY

Received: Mar. 16, 2023

Accepted: July 07, 2023

KEYWORDS

Green synthesis,
ZnO NPs,
Laurus nobilis leaf,
Antiproliferative activity,
Antibacterial activity

1. INTRODUCTION

ZnO NPs, due to their superior properties, namely large binding energy, wide band gap, and high piezoelectricity, have many applications such as medical imaging (Lim *et al.*, 2012; Senthilkumar *et al.*, 2009), nanocomposites (Bhattacharya & Samanta, 2016), drug delivery (Yuan *et al.*, 2010), and hyperthermia of tumors (Sharma *et al.*, 2022). There are numerous methods to synthesize ZnO NPs, including mechanical grinding, chemical reduction, laser cutting, photoreduction, and the green approach (Agarwal *et al.*, 2017; Ghimire *et al.*, 2022; Wirunchit *et al.*, 2021). Among them; the green approach is of great interest to reduce metal salts to nanoparticles because it is inexpensive, non-toxic, and environmentally friendly (Jadoun *et al.*, 2021). There are many studies in the literature on the synthesis of ZnO NPs using different plant extracts such as *Nephelium lappaceum* L. (Karnan & Selvakumar, 2016) *Mangifera indica* (Rajeshkumar *et al.*, 2018), *Suaeda aegyptiaca* (Rajabi *et al.*, 2017), *Calotropis gigantea*

*CONTACT: Firdevs MERT SİVRİ  firdevssivri@sdu.edu.tr  Suleyman Demirel University, Department of Basic Pharmaceutical Sciences, 32200 Isparta, Türkiye

(Vidya *et al.*, 2013), *Aspalathus linearis* (Diallo *et al.*, 2015), and *Syzygium Cumini* (Sadiq *et al.*, 2021). Synthesis of nanoparticles from plant extracts is a bottom-up approach using metal salts as precursors (Hoda *et al.*, 2021).

L. nobilis is an evergreen, aromatic plant of the Lauraceae family that grows in temperate and tropical areas of the world, including Türkiye, Spain, Morocco, Greece, Portugal, Mexico, and other Mediterranean nations (Alejo-Armijo *et al.*, 2017). The leaves of this plant are used as a spice flavoring in foods. In addition, leaf extracts are used for fungal and antimicrobial infections, and to treat burping, bloating, and gastrointestinal issues (A. Sharma *et al.*, 2012). *L. nobilis* leaf extract contains ingredients such as sugars, kaempferol glycosides, sesquiterpene lactones, megastigme glycosides, organic acids, (+)-catechin, (+)-gallocatechin, (+)-epigallocatechin, (-)-epicatechin, and procyanidins (Kaurinovic *et al.*, 2010). Thanks to the components it contains, the plant can form and stabilize nanoparticles by reducing metallic ions (Rai *et al.*, 2009).

Cancer, which is the primary cause of death worldwide, is one of the health problems that most concern and affect society. In 2020, colorectal cancer was the third cause of cancer-related death in the United States (Siegel *et al.*, 2020). Depending on the type of cancer, its stage, and the patient's health, several treatment methods, including surgery, radiotherapy, and chemotherapy, are used (Debela *et al.*, 2021). However, these treatment methods have disadvantages such as selectivity, multi-drug resistance, and adverse side effects (Mondal *et al.*, 2014). Recently, nanoparticles' small size and greater atomic content on their surface allow them to interact with biomolecules both inside and outside body cells, enabling them to be used in medicine to treat cancer as drug delivery systems and diagnostic tools (Mundekkad & Cho, 2022; Zabielska-Koczywąs & Lechowski, 2017).

In this study, *L. nobilis* leaf extract was used to synthesize ZnO NPs. The synthesized ZnO NPs were characterized by UV-Vis spectroscopy, XRD, FTIR, and TEM. *S. aureus* and *E. coli* strains were utilized to examine the antibacterial activity of ZnO NPs. In addition, the Minimum Inhibitory Concentration (MIC)-Minimum Bactericidal Concentrations (MBC) of ZnO NPs were determined. The antiproliferative activity of ZnO NPs was tested against a human colon cancer cell line and a mouse normal fibroblast cell line using MTT assay in vitro.

2. MATERIAL and METHODS

2.1. Chemical Used

Zinc acetate dihydrate ($\text{Zn}(\text{CH}_3\text{CO}_2)_2 \cdot 2\text{H}_2\text{O}$) and Sodium hydroxide (NaOH) used in this study were purchased from Merck Company. Deionized water was used throughout the experimental study. *L. nobilis* leaves were collected from the Antalya region and their type has been confirmed.

2.2. Preparation of Aqueous Leaf Extract

L. nobilis leaves were washed with tap water and then with deionized water to purify them from dust and foreign wastes and dried them by laying in the shade at room conditions. After the dried *L. nobilis* leaves were ground, the powder was sieved with a particle size of 0.630 – 1.00 mm to be used in the extract. 2.5 g of powdered *L. nobilis* leaves and 100 ml of deionized water were taken into a 250 ml flask and boiled under reflux for 5 min. Then, the extract was cooled to room temperature and filtered. The extract was centrifuged at 9500 rpm for 5 minutes to remove plant residues and impurities and kept at 4°C for further studies.

2.3. Synthesis of Nanoparticles

Zinc acetate dihydrate was used as a metal precursor for the synthesis of ZnO NPs. ZnO NPs were synthesized using *L. nobilis* leaf extract with minor modification, as previously demonstrated by Dönmez (Dönmez, 2021). 10 ml of *L. nobilis* leaf extract was added to 90 ml

of 0.02 M zinc acetate solution and stirred at room temperature using a magnet stirrer. Then, 1 M NaOH was added drop by drop to reach the pH of the mixture to 12 and the solution was stirred at room temperature for 2 hours. The resulting white mixture was centrifuged at 9500 rpm for 30 min. The precipitate was purified with deionized water and ethanol to remove impurities. Finally, obtained white precipitate was dried at 60° overnight and then calcined at 200°C for 3 hours.

2.4. Characterization of Synthesized Nanoparticles

ZnO NPs were characterized by UV-Vis spectroscopy, XRD, FTIR, and TEM techniques. UV-visible spectra of ZnO NPs were recorded in the 200 to 700 nm wavelength range using a JASCO V-770 UV/Vis spectrometer operating at a 1 nm resolution. X-ray diffractometer with Cu Ka radiation wavelength of 0.15406 nm investigated the phase structure and material identification of ZnO NPs. Spectrum was obtained using Panalytical Empyrian X-ray diffractometry at an angle of 2θ in the range of 10° to 80°. The morphologies and dimensions of ZnO NPs were investigated by Transmission Electron Microscopy (JEOL JEM-1010). The stability of synthesized ZnO NPs was measured by zeta potential analysis (Horiba Scientific).

2.5. Bacterial Strains and Determination of Minimum Inhibitory Concentration (MIC)-Minimum Bactericidal Concentration (MBC)

To investigate the antibacterial activity of ZnO NPs Gram-positive *S. aureus* ATCC 25923, and Gram-negative, *E. coli* ATCC 25922 strains were used. The bacteria strains were cultured in Mueller Hinton broth (MHB) (Merck, Germany) at 37°C for 18-24 h with 120 rpm.

The detection of MIC of ZnO NPs was carried out using a microtitre broth dilution method. The bacterial suspension was adjusted with sterile saline to a concentration of 10^8 CFU ml⁻¹. A hundred μL of ZnO NPs were added to the wells containing 100 μL MHB medium and serially diluted two-fold. Five μL of bacterial suspension adjusted to 0.5 McFarland inoculated each well and plates were incubated at 37 °C for 24 h. Following incubation, microplates were evaluated. The smallest concentration without growth was determined as the MIC value. MBC test was performed by plating the suspension from each well of microtiter plates into the MHA plate. The plates were incubated at 37°C for 24 h. The lowest concentration with no visible growths on the MHA plate was taken as the MBC value.

2.6. Investigation of the Effects of ZnO NPs Against Colon Cancer Cell Line and Mouse Adipose Fibroblast Cell Line

The human colon adenocarcinoma epithelial cell line (DLD-1) (ATCC® CCL-221TM) was purchased from the American Type Culture Collection (ATCC, USA). Mouse adipose fibroblast cell line (L929) (ATCC® CCL-1TM) was donated by Associate Professor Cigdem Yucel from Erciyes University, Faculty of Pharmacy. DLD-1 and L929 cell lines were cultured in DMEM supplemented with 10% FBS and 1% glutamax. The cell seeding was done at 5×10^3 cells/well density into 96-well plates. The DLD-1 and L929 cells were exposed to ZnO NPs at 50, 25, 12.5, 6.25, and 3.125 μL/mL concentrations for 48 h. The 50 μL of MTT stock solution, which is prepared as 5 mg/mL in DMEM solution, was added to the plate wells and, were incubated for 3 h. Absorbance values were measured in an Elisa plate reader at 590 nm.

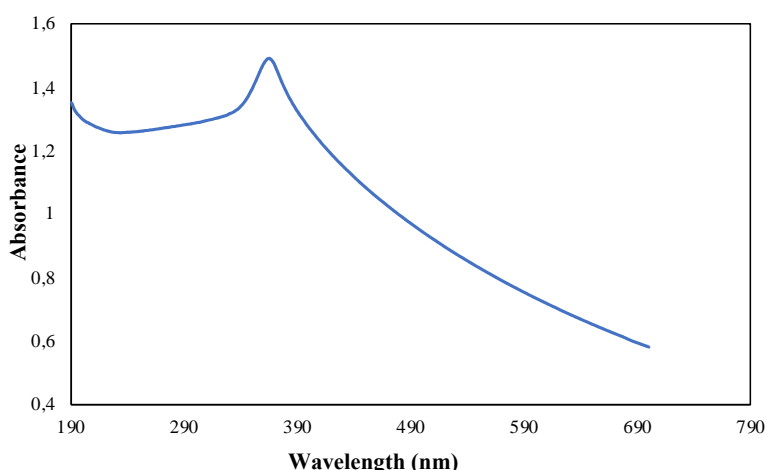
3. RESULTS and DISCUSSION

3.1. Characterization of ZnO NPs

In this study, the synthesis of ZnO NPs using *L. nobilis* leaf extract was successfully carried out. Firstly, UV-Vis analysis was performed to observe the formation of synthesized ZnO NPs. The UV-Vis spectrum of ZnO NPs is given in [Figure 1](#) and the absorption peak at 372 nm belongs to the SPR absorption of it. The structure of the plasmon band and the wavelength

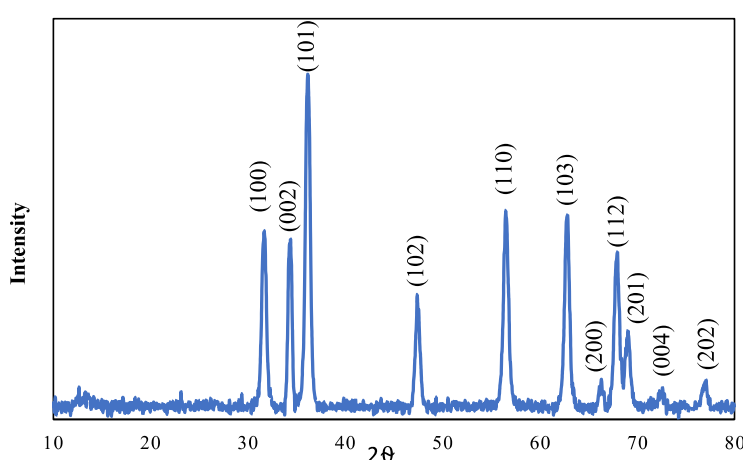
range in which it is observed vary according to the size distribution, average diameter, and shape of the nanoparticles (Link & El-Sayed, 1999). It is well known that the plasmon band gap in the UV-Vis Spectrum of ZnO NPs increases with decreasing particle size. For example, Hammad *et al.* (2010) investigated the change in particle size by exposing the synthesized ZnO NPs to different calcination temperatures and reported that there is a change in the plasmon band depending on the particle size in the UV-Vis spectrum of ZnO NPs of different sizes (Hammad *et al.*, 2010).

Figure 1. UV-Vis spectrum of synthesized ZnO NPs.



The crystal structure of the synthesized ZnO NPs was determined by XRD diffraction analysis. The XRD patterns of the synthesized ZnO NPs are given in [Figure 2](#). The XRD diffraction peaks of the synthesized ZnO NPs are in good agreement with the ZnO hexagonal wurtzite structure of the Joint Committee on Powder Diffraction Standards (JCPDS-36-1451). No characteristic diffraction peaks were observed in the XRD analysis except for ZnO, indicating that the ZnO NPs were free of unwanted impurities. Similar results have been reported in some studies in the literature (Al-Kordy *et al.*, 2021; Khorsand Zak *et al.*, 2011).

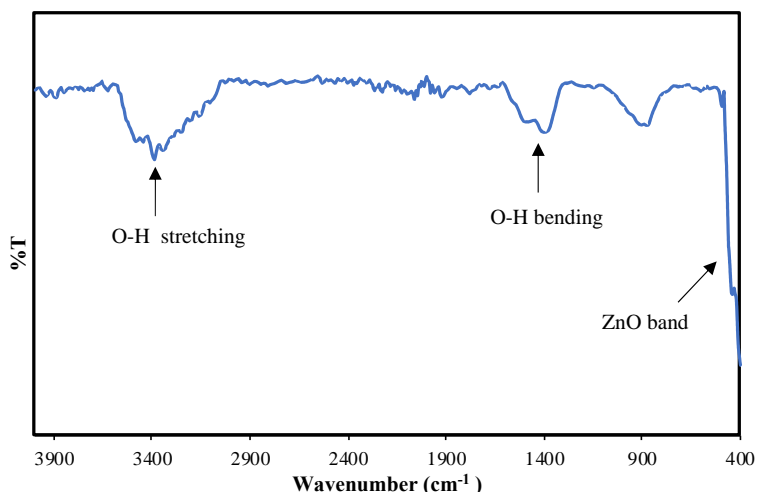
Figure 2. XRD pattern of synthesized ZnO NPs.



FTIR spectra of synthesized ZnO NPs were taken in the range of 400–4000 cm^{-1} as seen in [Figure 3](#). The characteristic stretching peak of the ZnO bond is assigned a significant vibration band in the FTIR spectrum ranging from 400 cm^{-1} to 500 cm^{-1} . A large peak at 3388 cm^{-1} (stretching) and 1670 cm^{-1} (bending), is caused by ambient moisture, indicating the presence of hydroxyl residue (Nagaraju *et al.*, 2017). The FTIR results are consistent with the results of

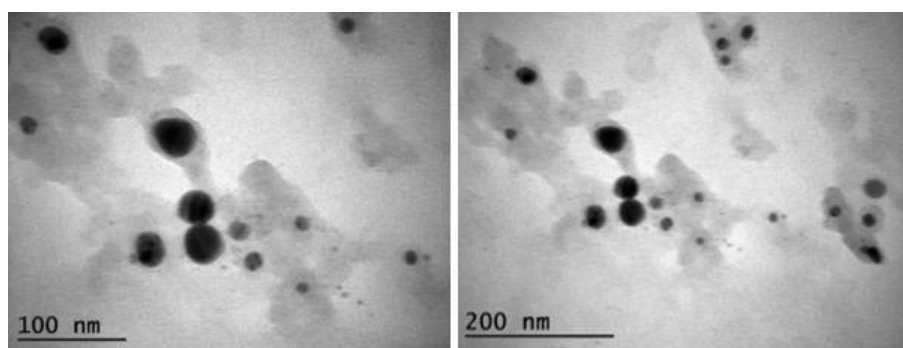
ZnO NPs which were synthesized from various plant extracts (Dobrucka & Długaszewska, 2016; Song & Yang, 2016).

Figure 3. FTIR spectra of synthesized ZnO NPs.



The TEM images of ZnO NPs synthesized using *L. nobilis* leaf extract, shown in [Figure 4](#), can help us analyze the size and shape of the synthesized nanoparticles. According to the TEM images of ZnO NPs, it was observed that the nanoparticles ranged in size from 9 to 33 nm, with a mean diameter of 16 ± 5 nm. It also showed that the synthesized ZnO NPs were roughly spherical.

Figure 4. TEM images of synthesized ZnO NPs.



The zeta potential analysis confirms the stability of ZnO NPs synthesized using *L. nobilis* leaf extract. As seen in [Figure 5](#), the zeta potential of the synthesized ZnO NPs is -25,2 mV. This result shows that the synthesized ZnO NPs are covered by negatively charged groups and are quite stable.

The size distributions of the synthesized ZnO NPs were examined by evaluating the TEM images with Adobe Photoshop 7. A total of 100 particles were counted and the size distribution plot for the corresponding particles is given in [Figure 6](#). The results show that the size of the synthesized ZnO NPs is between 9 nm and 33 nm.

Figure 5. Zeta potential of synthesized ZnO NPs.

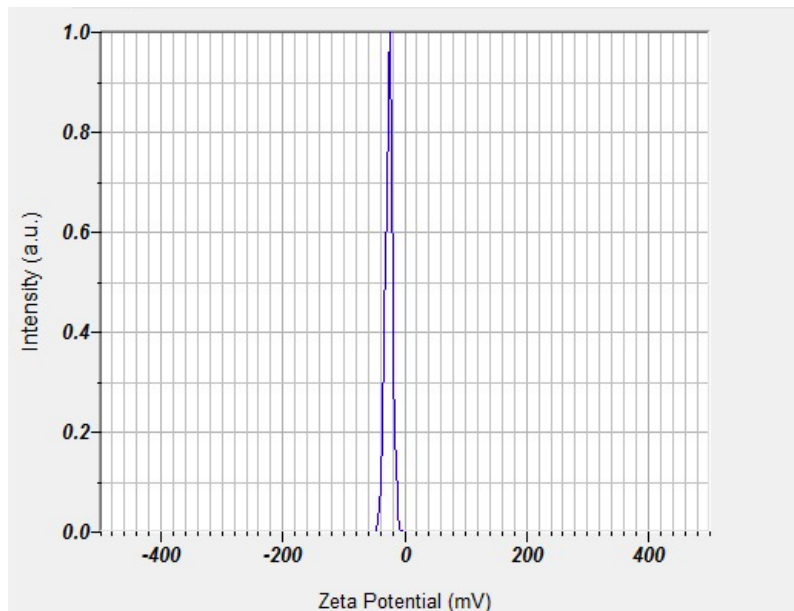
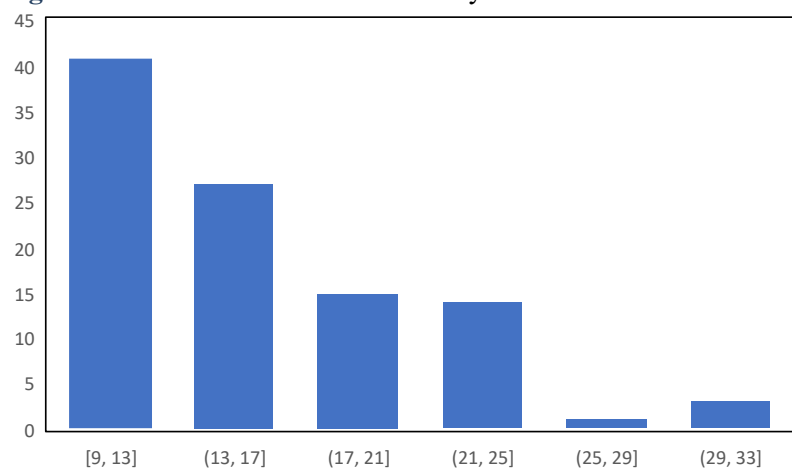


Figure 6. Particles size distribution of synthesized ZnO NPs.



3.2. Bacterial strains and Determination of MIC- MBC of ZnO NPs

Since ancient times, people have utilized the antibacterial properties of certain metals and their ions. Today, it is known that a variety of metals, including Ag, Al, Co, Cu, Fe, Ga, Mn, Ni, Pb, and Zn, have antibacterial properties (Gudkov *et al.*, 2021). The capacity of metal ions to block enzymes, disrupt cell membranes, hinder the uptake of critically needed microelements by microorganisms, or induce DNA damage forms the basis of metals' antimicrobial activity (Turner, 2017). The MIC/ MBC results against the test bacteria are given in [Table 1](#). The results showed that the ZnO NPs had antibacterial activity and the MBC and MIC of *S. aureus* and *E. coli* were 4,35 mg/mL and 2,175 mg/mL, respectively. The antibacterial activity of the *L. nobilis* leaf extract on bacteria was not observed at the studied concentration. The antibacterial effect of ZnO NPs has been demonstrated in many studies carried out so far (Anand *et al.*, 2019; D. Sharma *et al.*, 2010). The physical and morphological characteristics of nanoparticles and synthesis techniques change their antibacterial capabilities. For example, Upadhyaya *et al.* (2018) reported that hexagonal ZnO NPs synthesized using *Lawsonia inermis* extract showed higher antibacterial activity against *S. aureus* than rod-shaped ZnO NPs at 100, 200, and 500 µg/mL concentrations. They concluded that hexagonal ZnO NPs, due to their shape,

penetrate the cell membrane barrier more easily than rod ZnO NPs and cause cell death (Upadhyaya *et al.*, 2018).

ZnO NPs show a higher antibacterial effect compared to bulk ZnO (Yamamoto, 2001). The factors that most affect the antibacterial activity of ZnO NPs are their small size and large surface/volume ratio. Akbar *et al.* (2017) reported that as the size of ZnO NPs decreases, the antibacterial effect increases (Akbar *et al.*, 2017). The smaller nanoparticles effectively penetrate through the cell walls of the bacteria, causing membrane damage and ultimately leading to cell lysis. The high antibacterial effect of the synthesized ZnO NPs can be attributed to their small size and hexagonal structure.

Table 1. Antibacterial activity of ZnO NPs against microorganisms (MIC/MBC value).

Microorganisms	ZnO NPs
<i>S. aureus</i> ATCC 25923	2.175/1.08
<i>E. coli</i> ATCC 25922	2.175/4.35

3.3. Antiproliferative Activity Studies of ZnO NPs

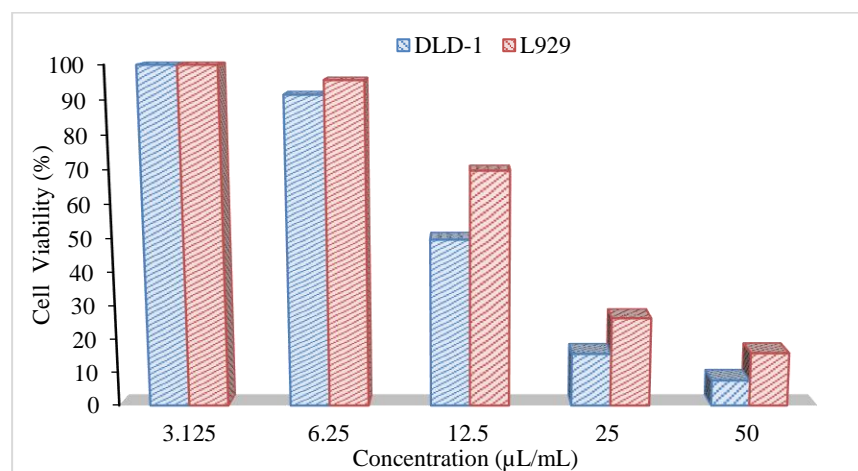
The synthesized ZnO NPs were tested in human colon cancer cell lines and mouse fibroblast cell lines *in vitro*. The results are given in [Table 2](#).

Table 2. IC₅₀ results of ZnO NPs in DLD-1 and L929 cell lines.

Compound	IC ₅₀ (μ L/mL)	
	DLD-1	L929
ZnO NPs	13.85	20.08

The results show that ZnO NPs have obvious antiproliferative activity in the colon cancer cell line with the half maximal inhibitory concentration (IC₅₀) value of 13.85 μ L/mL for 48 h. From the above IC₅₀ value, it is clearly seen that the synthesized ZnO NPs can inhibit the growth of colon cancer cells. It was also determined from the cell culture studies that the synthesized ZnO NPs showed selectivity on healthy cells (L929) and IC₅₀ value was obtained as 20.08 μ L/mL. The normal and cancer cell viability ratios depending on concentrations of ZnO NPs are given in [Figure 7](#).

Figure 7. Changing cell viability rates depending on the concentrations of synthesized ZnO NPs.



It is seen that the synthesized ZnO NPs has an effect on cell viability depending on the concentration ([Figure 7](#)). At 3.125 μ L/mL concentration, the ZnO NPs was found to be inactive on both healthy (L929) and cancerous (DLD-1) cells. In the colon cancer cell line, it is seen

that the cell viability rates interacting with the ZnO NPs decreased by 91.57%, 49.88%, 15.74%, 7.64% for 6.25, 12.5, 25 and 50 $\mu\text{L}/\text{mL}$, respectively, as the concentration increased. It is clearly seen that the synthesized ZnO NPs at 12.5 μM have selectivity on healthy cells and the viability rates were obtained as 49.88% and 69.93% for DLD-1 and L929, respectively. At 50 $\mu\text{L}/\text{mL}$ of the ZnO NPs, the viability of healthy cells was almost twice that of cancer cells at 15.95%.

4. CONCLUSION

In this study, ZnO NPs were successfully synthesized from *L. nobilis* leaves extract via the green approach, which is an inexpensive, non-toxic, and eco-friendly method. The synthesized ZnO NPs were characterized by UV, TEM, XRD, and FT-IR. According to XRD diffraction analysis of ZnO NPs, it was observed that they have a hexagonal wurtzite structure. The size and shape of the ZnO NPs were determined using the TEM method. According to the TEM images of ZnO NPs, it was observed that the nanoparticles ranged in size from 9 to 33 nm, with a mean diameter of 16 ± 5 nm. To investigate the antibacterial effect of ZnO NPs *S. aureus*, and *E. coli* strains were used. The MIC/MBC results of ZnO NPs against test bacteria showed that they had antibacterial activity and MBC and MIC values of *S. aureus* and *E. coli* were 4.35 mg/mL and 2.175 mg/mL, respectively. Bacterial infectious illnesses are a severe public health issue that has gained international attention as a hazard to human health that also has implications for the economy and society. Therefore, new antibacterial agents are needed to combat infectious diseases. Although the antibacterial effect of nanoparticles on many microorganisms is seen as a promising approach, more research is required on it.

In addition, synthesized ZnO NPs were screened in DLD-1 and L929 cell lines. The nanoparticles were found to be effective in DLD-1. Furthermore, it has selectivity against normal cell lines. Synthesized ZnO NPs have the potential to be used in biomedical applications thanks to their antibacterial and anticancer activity.

Acknowledgments

We would like to thank the Suleyman Demirel University Research Funds (TSG-2021-8458 and TLP-2022-8777) for financial support.

Declaration of Conflicting Interests and Ethics

The authors declare no conflict of interest. This research study complies with research and publishing ethics. The scientific and legal responsibility for manuscripts published in IJSM belongs to the authors.

Authorship Contribution Statement

Firdevs Mert Sivri, Cennet Çirrik, and Aleyna Ezer: Carried out the *L. nobilis* leaves extract and synthesis of ZnO NPs using *L. nobilis* leaf extract. **Ebru Önem:** Determined the antibacterial activity, and the Minimum Inhibitory Concentration (MIC)-Minimum Bactericidal Concentrations of ZnO NPs. **Senem Akkoç:** Tested the antiproliferative activity of ZnO NPs against a human colon cancer cell line and a mouse normal fibroblast cell line using the in vitro MTT assay. All authors wrote down the methods and discussion texts of the experiments they performed in the study. All authors reviewed the manuscript.

Orcid

Firdevs Mert Sivri  <https://orcid.org/0000-0002-0545-0268>
Ebru Önem  <https://orcid.org/0000-0002-7770-7958>
Senem Akkoç  <https://orcid.org/0000-0001-8913-757X>
Cennet Çirrik  <https://orcid.org/0009-0002-3361-4570>
Aleyna Ezer  <https://orcid.org/0009-0005-5629-8576>

REFERENCES

- Agarwal, H., Venkat Kumar, S., & Rajeshkumar, S. (2017). A review on green synthesis of zinc oxide nanoparticles – An eco-friendly approach. *Resource-Efficient Technologies*, 3(4), 406–413. <https://doi.org/10.1016/j.refit.2017.03.002>
- Akbar, S., Haleem, K.S., Tauseef, I., Rehman, W., Ali, N., & Hasan, M. (2017). *Raphanus sativus* Mediated Synthesis, Characterization and Biological Evaluation of Zinc Oxide Nanoparticles. *Nanoscience and Nanotechnology Letters*, 9(12), 2005–2012. <https://doi.org/10.1166/nnl.2017.2550>
- Alejo-Armijo, A., Altarejos, J., & Salido, S. (2017). Phytochemicals and biological activities of laurel tree (*Laurus nobilis*). *Natural Product Communications*, 12(5), 1934578X1701200519.
- Al-Kordy, H.M.H., Sabry, S.A., & Mabrouk, M.E.M. (2021). Statistical optimization of experimental parameters for extracellular synthesis of zinc oxide nanoparticles by a novel haloaliphilic Alkalibacillus sp.W7. *Scientific Reports*, 11(1), 10924. <https://doi.org/10.1038/s41598-021-90408-y>
- Anand, G.T., Renuka, D., Ramesh, R., Anandaraj, L., Sundaram, S.J., Ramalingam, G., Magdalane, C.M., Bashir, A., Maaza, M., & Kaviyarasu, K. (2019). Green synthesis of ZnO nanoparticle using *Prunus dulcis* (Almond Gum) for antimicrobial and supercapacitor applications. *Surfaces and Interfaces*, 17, 100376.
- Bhattacharya, S., & Samanta, S.K. (2016). Soft-Nanocomposites of Nanoparticles and Nanocarbons with Supramolecular and Polymer Gels and Their Applications. *Chemical Reviews*, 116(19), 11967–12028. <https://doi.org/10.1021/acs.chemrev.6b00221>
- Debela, D.T., Muzazu, S.G., Heraro, K.D., Ndalamu, M.T., Mesele, B.W., Haile, D.C., Kitui, S.K., & Manyazewal, T. (2021). New approaches and procedures for cancer treatment: Current perspectives. *SAGE Open Medicine*, 9, 205031212110343. <https://doi.org/10.1177/20503121211034366>
- Diallo, A., Ngom, B.D., Park, E., & Maaza, M. (2015). Green synthesis of ZnO nanoparticles by *Aspalathus linearis*: Structural & optical properties. *Journal of Alloys and Compounds*, 646, 425–430. <https://doi.org/10.1016/j.jallcom.2015.05.242>
- Dobrucka, R., & Długaszevska, J. (2016). Biosynthesis and antibacterial activity of ZnO nanoparticles using *Trifolium pratense* flower extract. *Saudi Journal of Biological Sciences*, 23(4), 517–523. <https://doi.org/10.1016/j.sjbs.2015.05.016>
- Dönmez, S. (2021). Green synthesis and characterization of zinc oxide nanoparticles by using *rhododendron ponticum* L. leaf extract. *Journal*, 4(1), 54–57.
- Ghimire, R.R., Parajuli, A., Gupta, S.K., & Rai, K.B. (2022). Synthesis of ZnO Nanoparticles by Chemical Method and its Structural and Optical Characterization. *BIBECHANA*, 19(1–2), 90–96. <https://doi.org/10.3126/bibechna.v19i1-2.46396>
- Gudkov, S.V., Burmistrov, D.E., Serov, D.A., Rebezov, M.B., Semenova, A.A., & Lisitsyn, A.B. (2021). A Mini Review of Antibacterial Properties of ZnO Nanoparticles. *Frontiers in Physics*, 9, 641481. <https://doi.org/10.3389/fphy.2021.641481>
- Hammad, T.M., Salem, J.K., & Harrison, R.G. (2010). The influence of annealing temperature on the structure, morphologies and optical properties of ZnO nanoparticles. *Superlattices and Microstructures*, 47(2), 335–340. <https://doi.org/10.1016/j.ultrami.2009.11.007>
- Hoda, N., Budama Akpolat, L., Mert SiVri, F., & Kurtuluş, D. (2021). Biosynthesis of Bimetallic Ag-Au (core-shell) Nanoparticles Using Aqueous Extract of Bay Leaves (*Laurus nobilis* L.). *Journal of the Turkish Chemical Society Section A: Chemistry*, 8(4), 1035–1044. <https://doi.org/10.18596/jotcsa.885558>
- Jadoun, S., Arif, R., Jangid, N.K., & Meena, R.K. (2021). Green synthesis of nanoparticles using plant extracts: A review. *Environmental Chemistry Letters*, 19(1), 355–374. <https://doi.org/10.1007/s10311-020-01074-x>

- Karnan, T., & Selvakumar, S.A.S. (2016). Biosynthesis of ZnO nanoparticles using rambutan (*Nephelium lappaceum L.*) peel extract and their photocatalytic activity on methyl orange dye. *Journal of Molecular Structure*, 1125, 358-365. <https://doi.org/10.1016/j.molstruc.2016.07.029>
- Kaurinovic, B., Popovic, M., & Vlaisavljevic, S. (2010). In Vitro and in Vivo Effects of *Laurus nobilis L.* Leaf Extracts. *Molecules*, 15(5), 3378-3390. <https://doi.org/10.3390/molecules15053378>
- Khorsand Zak, A., Razali, Abd Majid, W.H.B., & Darroudi, M. (2011). Synthesis and characterization of a narrow size distribution of zinc oxide nanoparticles. *International Journal of Nanomedicine*, 1399. <https://doi.org/10.2147/IJN.S19693>
- Lim, S.T., Jeong, H. jeong, Kim, D.W., Lim, S.T., Sohn, M.H., Lee, J.K., Jeong, J., & Lee, C.-M. (2012). Optical imaging to trace near infrared fluorescent zinc oxide nanoparticles following oral exposure. *International Journal of Nanomedicine*, 3203. <https://doi.org/10.2147/IJN.S32828>
- Link, S., & El-Sayed, M.A. (1999). Size and Temperature Dependence of the Plasmon Absorption of Colloidal Gold Nanoparticles. *The Journal of Physical Chemistry B*, 103(21), 4212–4217. <https://doi.org/10.1021/jp984796o>
- Mondal, J., Panigrahi, A., & Khuda-Bukhsh, A. (2014). Conventional chemotherapy: Problems and scope for combined therapies with certain herbal products and dietary supplements. *Austin J Mol Cell Biol*, 1(1), 1–10.
- Mundekkad, D., & Cho, W.C. (2022). Nanoparticles in Clinical Translation for Cancer Therapy. *International Journal of Molecular Sciences*, 23(3), 1685. <https://doi.org/10.3390/ijms23031685>
- Nagaraju, G., Udayabhanu, Shivaraj, Prashanth, S.A., Shastri, M., Yathish, K.V., Anupama, C., & Rangappa, D. (2017). Electrochemical heavy metal detection, photocatalytic, photoluminescence, biodiesel production and antibacterial activities of Ag-ZnO nanomaterial. *Materials Research Bulletin*, 94, 54-63. <https://doi.org/10.1016/j.materresbul.2017.05.043>
- Rai, M., Yadav, A., & Gade, A. (2009). Silver nanoparticles as a new generation of antimicrobials. *Biotechnology Advances*, 27(1), 76-83. <https://doi.org/10.1016/j.biotechadv.2008.09.002>
- Rajabi, H.R., Naghiha, R., Kheirizadeh, M., Sadatfaraji, H., Mirzaei, A., & Alvand, Z.M. (2017). Microwave assisted extraction as an efficient approach for biosynthesis of zinc oxide nanoparticles: Synthesis, characterization, and biological properties. *Materials Science and Engineering: C*, 78, 1109–1118. <https://doi.org/10.1016/j.msec.2017.03.090>
- Rajeshkumar, S., Kumar, S.V., Ramaiah, A., Agarwal, H., Lakshmi, T., & Roopan, S.M. (2018). Biosynthesis of zinc oxide nanoparticles using *Mangifera indica* leaves and evaluation of their antioxidant and cytotoxic properties in lung cancer (A549) cells. *Enzyme and Microbial Technology*, 117, 91–95. <https://doi.org/10.1016/j.enzmictec.2018.06.009>
- Sadiq, H., Sher, F., Sehar, S., Lima, E.C., Zhang, S., Iqbal, H.M.N., Zafar, F., & Nuhanović, M. (2021). Green synthesis of ZnO nanoparticles from *Syzygium Cumini* leaves extract with robust photocatalysis applications. *Journal of Molecular Liquids*, 335, 116567. <https://doi.org/10.1016/j.molliq.2021.116567>
- Senthilkumar, K., Senthilkumar, O., Yamauchi, K., Sato, M., Morito, S., Ohba, T., Nakamura, M., & Fujita, Y. (2009). Preparation of ZnO nanoparticles for bio-imaging applications. *Physica Status Solidi (b)*, 246(4), 885–888. <https://doi.org/10.1002/pssb.200880606>
- Sharma, A., Singh, J., & Kumar, S. (2012). Bay leaves. In *Handbook of herbs and spices* (pp. 73–85). Elsevier.
- Sharma, D.K., Shukla, S., Sharma, K.K., & Kumar, V. (2022). A review on ZnO: Fundamental properties and applications. *Materials Today: Proceedings*, 49, 3028–3035.

<https://doi.org/10.1016/j.matpr.2020.10.238>

- Sharma, D., Rajput, J., Kaith, B.S., Kaur, M., & Sharma, S. (2010). Synthesis of ZnO nanoparticles and study of their antibacterial and antifungal properties. *Thin Solid Films*, 519(3), 1224–1229. <https://doi.org/10.1016/j.tsf.2010.08.073>
- Siegel, R.L., Miller, K.D., Goding Sauer, A., Fedewa, S.A., Butterly, L.F., Anderson, J.C., Cercek, A., Smith, R.A., & Jemal, A. (2020). Colorectal cancer statistics, 2020. *CA: A Cancer Journal for Clinicians*, 70(3), 145–164. <https://doi.org/10.3322/caac.21601>
- Song, Y., & Yang, J. (2016). Preparation and *in-vitro* cytotoxicity of zinc oxide nanoparticles against osteoarthritic chondrocytes. *Tropical Journal of Pharmaceutical Research*, 15(11), 2321. <https://doi.org/10.4314/tjpr.v15i11.4>
- Turner, R.J. (2017). Metal-based antimicrobial strategies. *Microbial Biotechnology*, 10(5), 1062–1065. <https://doi.org/10.1111/1751-7915.12785>
- Upadhyaya, H., Shome, S., Sarma, R., Tewari, S., Bhattacharya, M.K., & Panda, S.K. (2018). Green synthesis, characterization and antibacterial activity of ZnO nanoparticles. *American Journal of Plant Sciences*, 9(6), 1279–1291.
- Vidya, C., Hiremath, S., Chandraprabha, M., Antonyraj, M., Gopal, I.V., Jain, A., & Bansal, K. (2013). Green synthesis of ZnO nanoparticles by Calotropis gigantea. *Int J Curr Eng Technol*, 1(1), 118–120.
- Wirunchit, S., Gansa, P., & Koetniyom, W. (2021). Synthesis of ZnO nanoparticles by Ball-milling process for biological applications. *Materials Today: Proceedings*, 47, 3554–3559. <https://doi.org/10.1016/j.matpr.2021.03.559>
- Yamamoto, O. (2001). Influence of particle size on the antibacterial activity of zinc oxide. *International Journal of Inorganic Materials*, 3(7), 643–646. [https://doi.org/10.1016/S1466-6049\(01\)00197-0](https://doi.org/10.1016/S1466-6049(01)00197-0)
- Yuan, Q., Hein, S., & Misra, R. (2010). New generation of chitosan-encapsulated ZnO quantum dots loaded with drug: Synthesis, characterization and *in vitro* drug delivery response. *Acta Biomaterialia*, 6(7), 2732–2739.
- Zabielska-Koczywąs, K., & Lechowski, R. (2017). The Use of Liposomes and Nanoparticles as Drug Delivery Systems to Improve Cancer Treatment in Dogs and Cats. *Molecules*, 22(12), 2167. <https://doi.org/10.3390/molecules22122167>